

PY502I - 8 Examples

J. M. D. Coey

School of Physics and CRANN, Trinity College Dublin

Ireland.

1. Active sensor bearing
2. Magnetocardiography
3. Mixed sensors
4. Magnetic barcodes
5. Security tags



Comments and corrections please: jcoey@tcd.ie

www.tcd.ie/Physics/Magnetism

8.1 Active sensor bearing

A magnetic tunnel junction (MTJ) sensor built into a roller bearing which is able to measure precisely the speed of rotation of a wheel. Used in antilock braking systems (ABS)

- Based on a MTJ sensor developed at Spintec, a research and development laboratory belonging to the French Atomic Energy Commission, associated with the University of Grenoble
- Developed by a small company (SNR)
- Destined for a mass-market application



Le prix Yves Rocard 2010 de la Société Française de Physique



Sensor holder



Drive wheel bearing

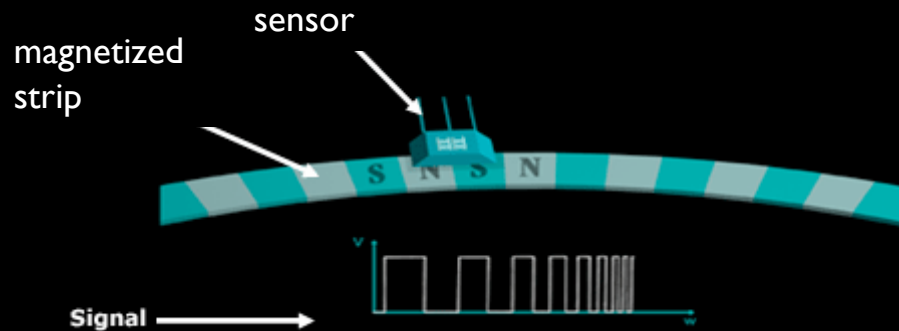


Non-drive wheel bearing

Magnetic encoder

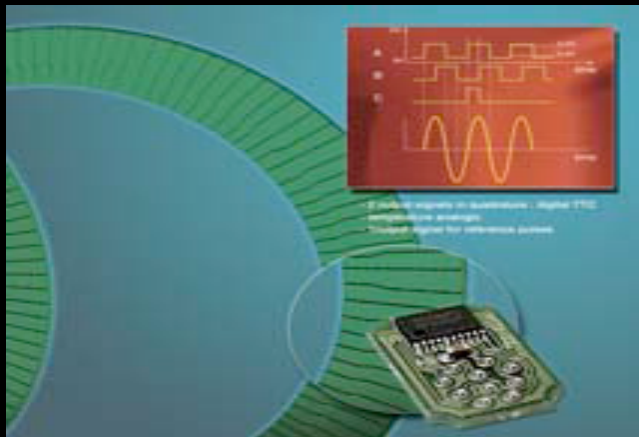
ASB Technology (Active Sensor Bearing)

First generation



reads velocity down to $v=0$
Avoids the wheels locking
Economical and compact solution
Simplified assembly
Global standard

Second generation

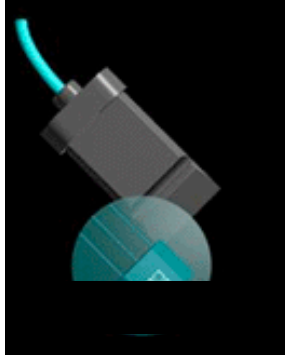


Measures position
and angular velocity
(marketed 2008)

SNR make 80 000 ASB bearings a day/

For the last 5 years, ten
of the most popular
vehicles in Europe have
been equipped with ASB

Design brief



Replace the first generation of field sensors by a linear sensor based on MTJ technology.

- Range of field measured ± 1.5 mT
- Operating temperature range
- Low power consumption
- Linear response
- Improved sensitivity

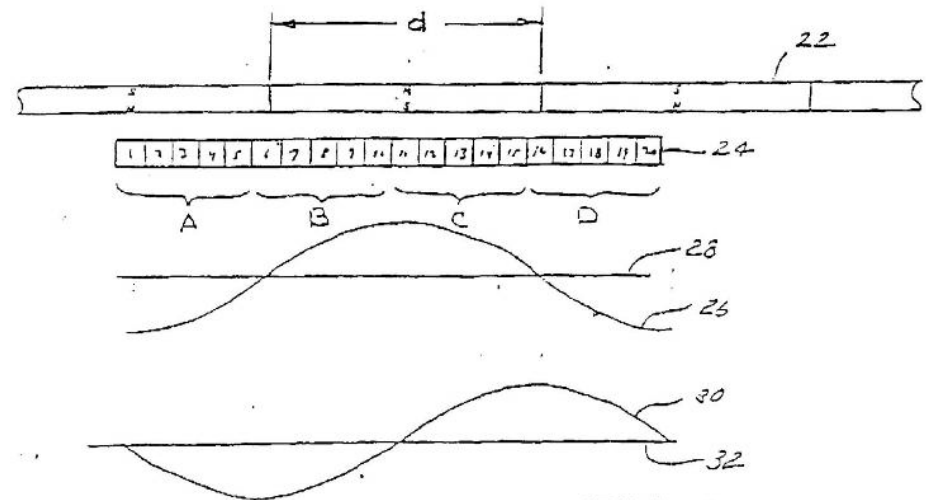
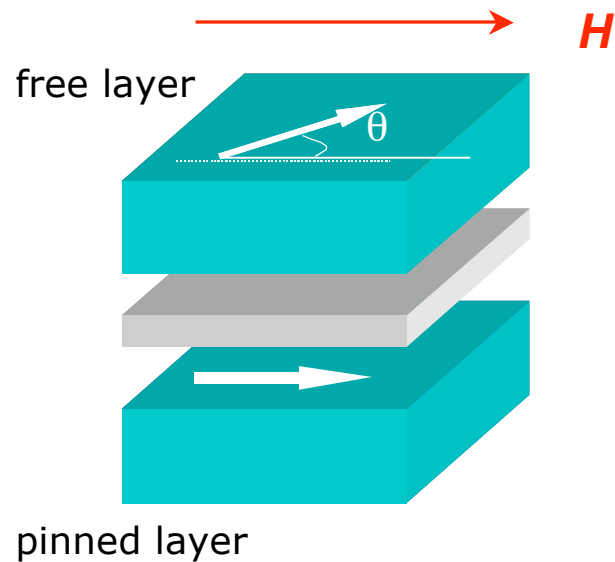


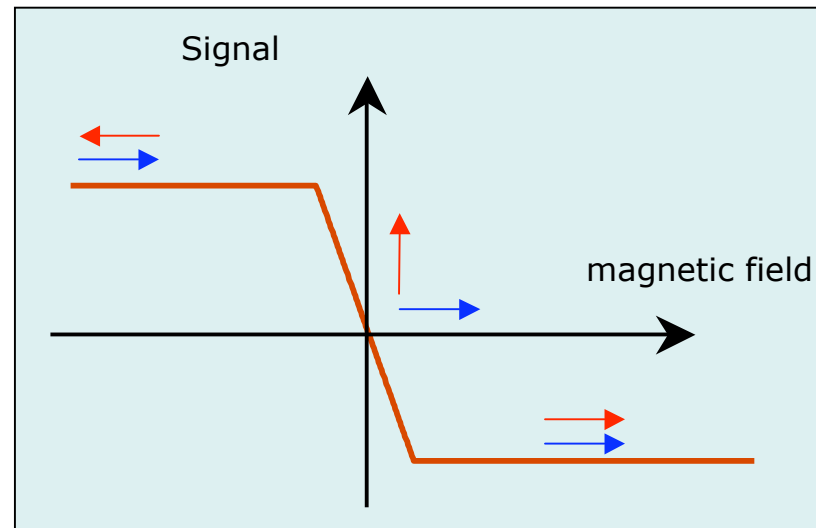
FIG. 2

MTJ sensor



- Two ferromagnetic layers separated by an insulator
- Free layer orientation controlled by magnetic field
- Tunnel current measured perpendicular to the plane

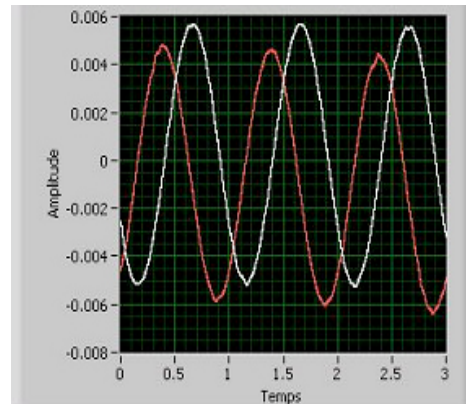
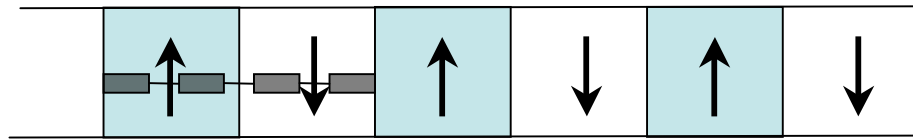
$$R \approx R_0 + \frac{\Delta R}{2} \cos \theta$$



key issue : control the magnitude and direction of the anisotropy

From tunnel junction to sensor

A sensor formed from four sensors, each separated by 1/4 of the magnetic period



- speed of rotation
- direction of rotation
- Position of the wheel
(count or use two tracks with different periods)

several sensors
+
Vernier effect 11/12



4096 points
per revolution



US 20070159164A1

(19) **United States**

(12) **Patent Application Publication** (10) **Pub. No.: US 2007/0159164 A1**

Hehn et al. (43) **Pub. Date: Jul. 12, 2007**

(54) **MAGNETORESISTIVE SENSOR,
COMPRISING A
FERROMAGNETIC/ANTIFERROMAGNETIC
SENSITIVE ELEMENT**

(30) **Foreign Application Priority Data**

Mar. 14, 2003 (FR)..... 03/03189
Sep. 16, 2003 (FR)..... 03/50545

Publication Classification

(76) Inventors: **Michel Hehn**, Neufves Maisons (FR);
Alain Schuhl, Nancy (FR); **Gregory
Malinowski**, Nancy (FR); **Christophe
Nicot**, Quintal (FR); **Christophe Duret**,
Annecy (FR)

(51) **Int. Cl.**
G01R 33/09 (2006.01)

(52) **U.S. Cl.** 324/207.21

(57) **ABSTRACT**

The invention concerns a magnetoresistive magnetic field sensor comprising a stack (1) of a reference element (2), a separation element (3) and an element (4) sensitive to the magnetic field, in which the reference element (2) and the sensitive element (4) have respectively a first and a second magnetic anisotropy (5, 6) in a first and a second direction. The sensitive element (4) comprises the superposition of a layer of a ferromagnetic material (FM1) and a layer of an antiferromagnetic material (AF1) which is arranged in order to obtain a magnetic moment (10) whose component oriented in the direction of the field to be measured varies reversibly in relation to the strength of the magnetic field to be measured, and linearly in an adjustable field range. The invention also concerns a use of such a sensor.

Correspondence Address:

ARENT FOX PLLC
1050 CONNECTICUT AVENUE, N.W.
SUITE 400
WASHINGTON, DC 20036 (US)

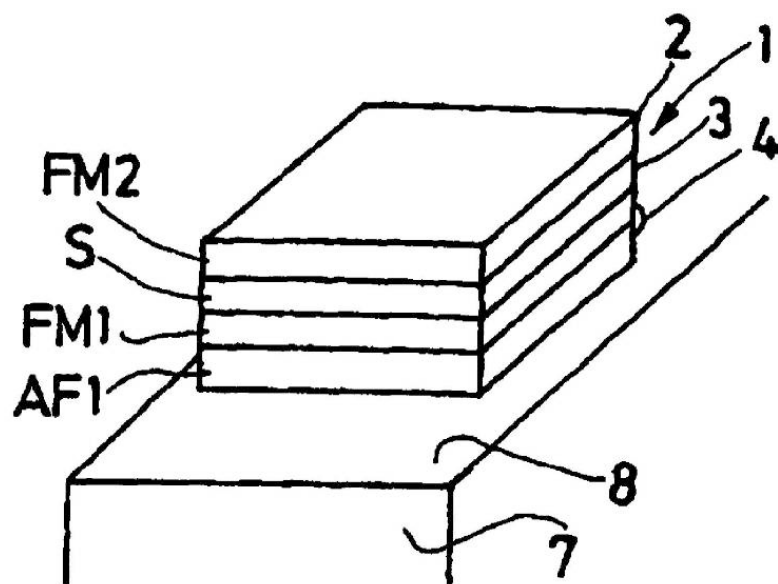
(21) Appl. No.: **10/548,604**

(22) PCT Filed: **Mar. 10, 2004**

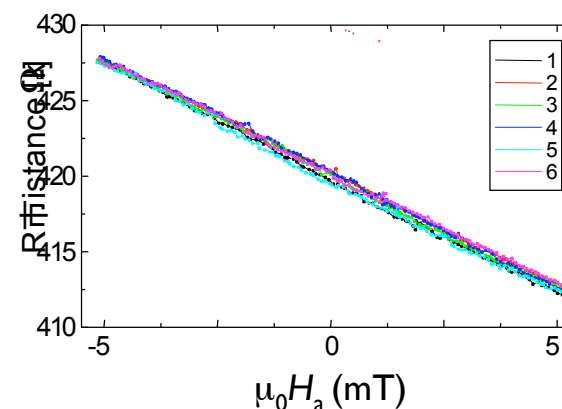
(86) PCT No.: **PCT/FR04/00574**

§ 371(c)(1),

(2), (4) Date: **May 17, 2006**



Linear response



$$R = R_0 + \frac{\Delta R}{2} \cos \theta$$

$$\cos \theta \approx \frac{H_a}{H_{eff}} \Rightarrow R \approx R_0 + \frac{\Delta R}{2} \cdot \frac{H_a}{H_{eff}}$$

Consider the response to a field applied in the x-direction,
which is the direction of the pinned, reference layer
Torque is zero on the free layer in equilibrium.

$$E = M_f H \cos \theta + M_f H_{eb} \sin \theta + K_u \sin^2 \theta$$

$$dE/d\theta = 0$$

$$0 = -M_f H \sin \theta + M_f H_{eb} \cos \theta + 2K_u \sin \theta \cos \theta$$

Since $\theta \approx \pi/2$, $\sin \theta \approx 1$, $\cos \theta$

$$\cos \theta = M_f H / [M_f H_{eb} + 2K_u]$$

$$R = R_0 + \{ \Delta R M_f / 2 [M_f H_{eb} + 2K_u] \} H - \text{linear in } H$$

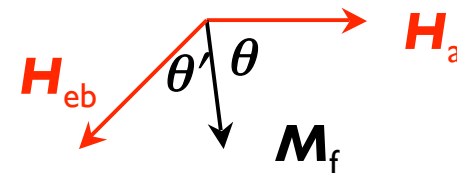
When $K_u \ll M_f H_{eb}$.

$$R = R_0 + (\Delta R / 2) H / H_{eb}$$

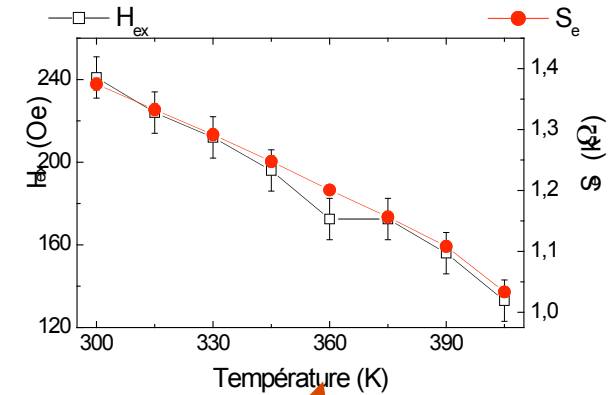
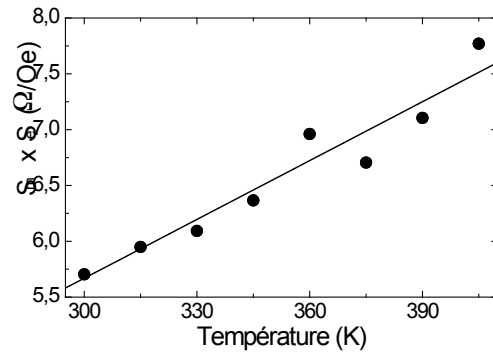
Pinned layer Co

AlO_x

Free layer Co/IrMn



Thermal drift



$$R = R_0 + \frac{\Delta R}{2} \cdot \frac{H_a}{H_{eb}}$$



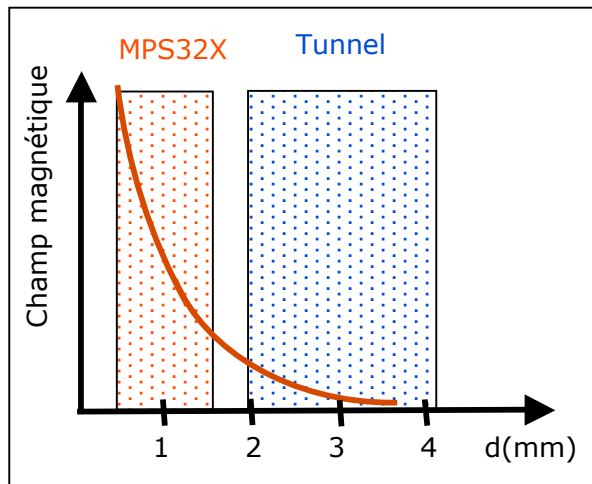
Temperature variation < 0.01% K⁻¹

Exchange bias decreases with temperature, but the deflection of the free layer increases correspondingly.

From a sensor to a product

Phase 1 Produce a laboratory demonstrator

Graduate student
G. Malinowski 2006

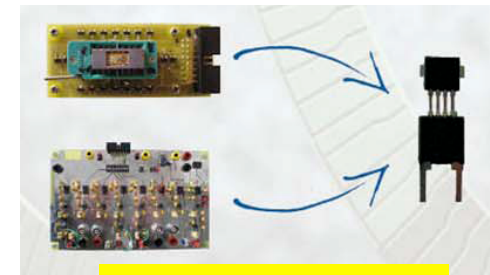


- Improved sensitivity
 - increase the distance from the magnet from 1 to 3 mm
 - raise the tolerances for sensor position
 - Use a cheaper magnet
- Electrical power consumption reduced by a factor 100
- Wider temperature range
- Improved signal/noise ratio

Phase 2 Develop an industrial process

Make the sensor in an industrial fab

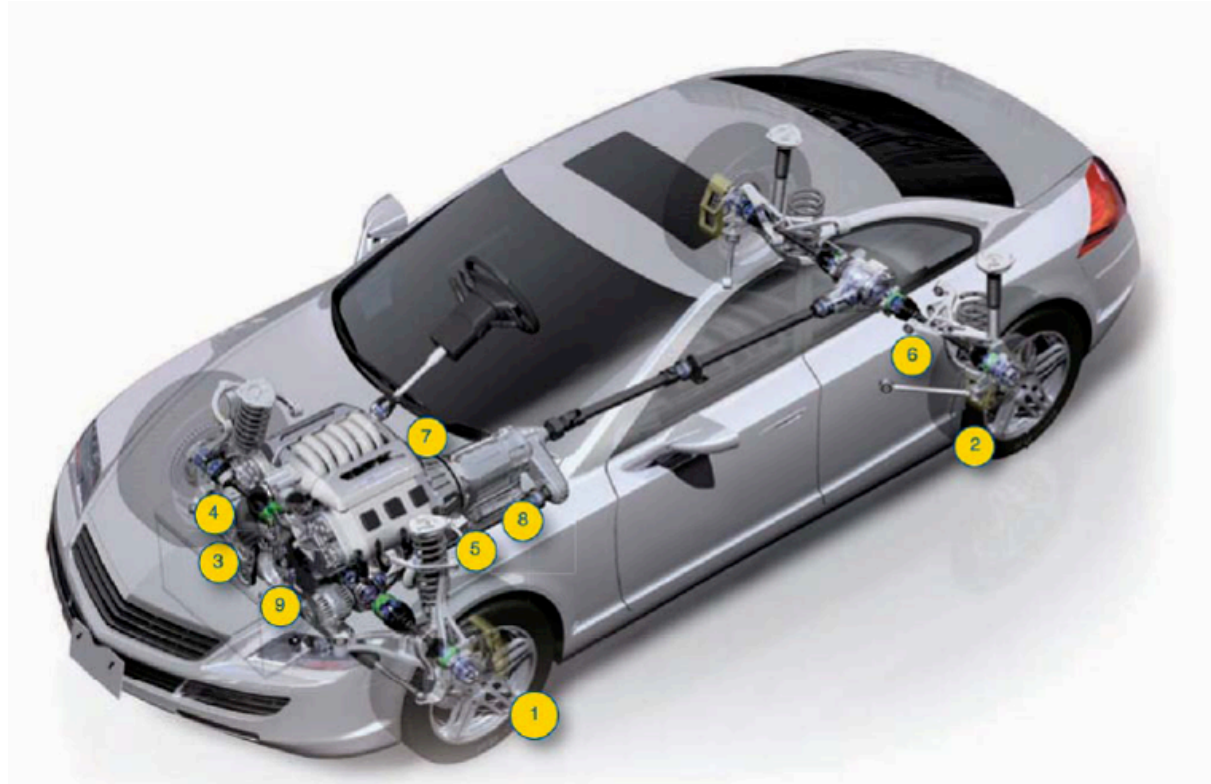
Produce an integrated prototype



CAMEL
project

Phase 3 Manufacture

Product to market
late 2012



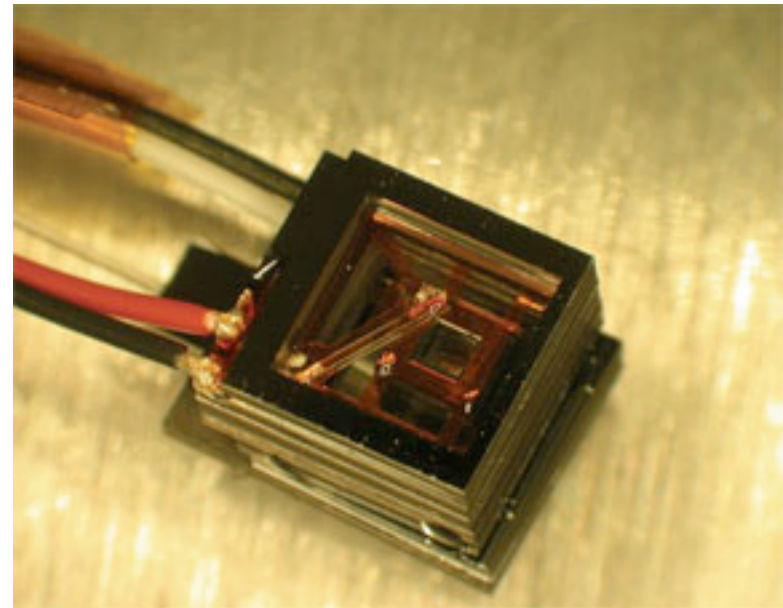
8.2 Heart sensor

A miniature Rb vapour magnetometer was developed at NIST. It uses a small ~ 4 mm cell containing 10^{11} Rb atoms, and a low-power laser.

The sensor is able to record the cardiac activity of a subject at a distance of 5 mm above the left side of the chest. Fields are of order pT from the heartbeat.

The device was tested in the magnetically-shielded room in Berlin. While not as sensitive as a SQUID, the device shows that alkali vapour magnetometers can be miniaturized, and operate in ambient conditions.

Another biomedical application is magnetic relaxometry, where magnetic nanoparticles are localized and imaged in the body via their transient magnetic relaxation.



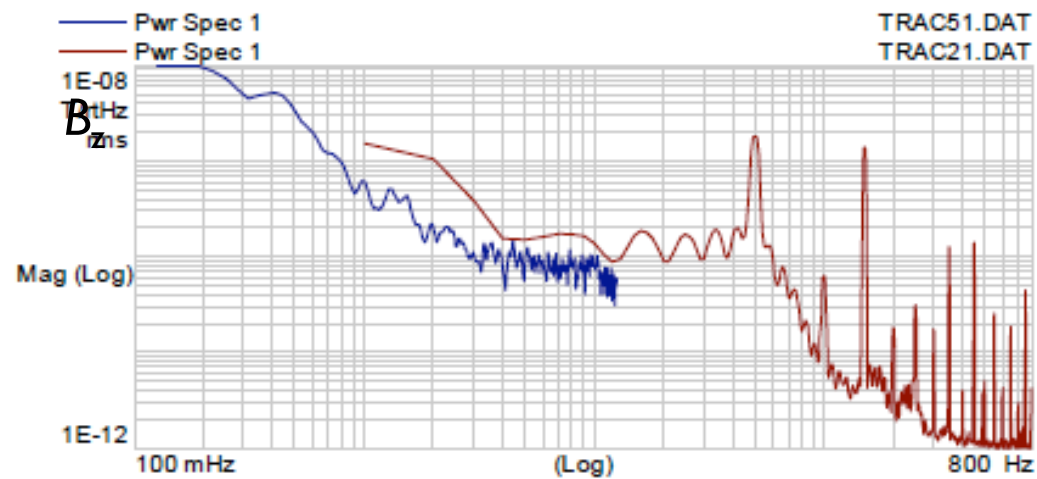
NIST's miniature magnetic sensor is about the size of a sugar cube. The lid has been removed to show the inner square cell, which contains a gas of rubidium atoms. The diagonal bar is an electrical connection to the cell's heaters, which are powered by the red, black and white electrical wires. The clear optical fiber extending from the middle bottom of the sensor connects to a control box. Credit: S. Knappe/NIST

Magnetically-shielded room at PTB, Berlin (Physikalisch Technische Bundesanstalt)

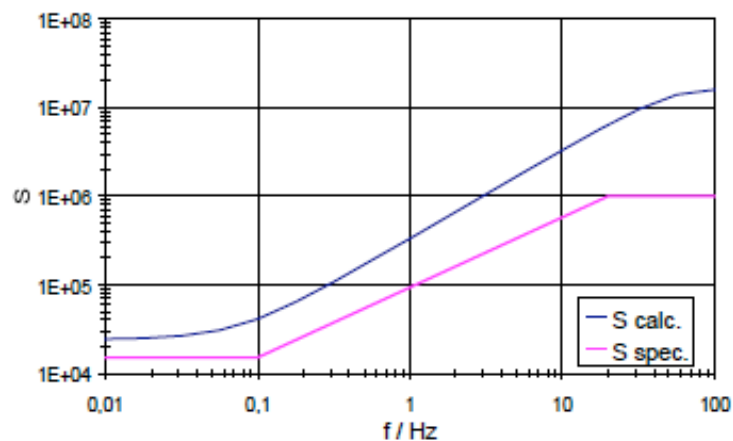


Aim: Achieve noise levels $\approx 1 \text{ fT}/\sqrt{\text{Hz}}$ in the range $0.001 - 500 \text{ Hz}$.
Ambient noise in the city is $\sim \text{nT}/\sqrt{\text{Hz}}$ at 1 Hz . A shielding factor $S > 10^6$ is needed.

7 layers of mumetal, one of Al (10mm, eddy current) + active shielding.

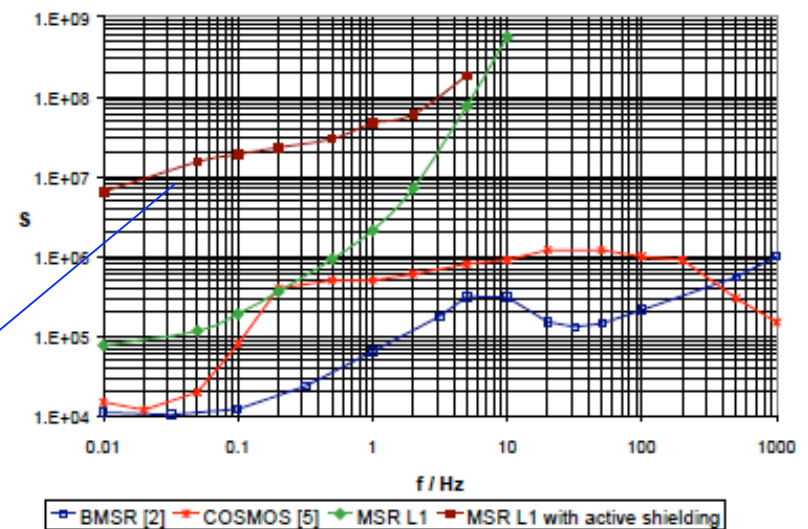
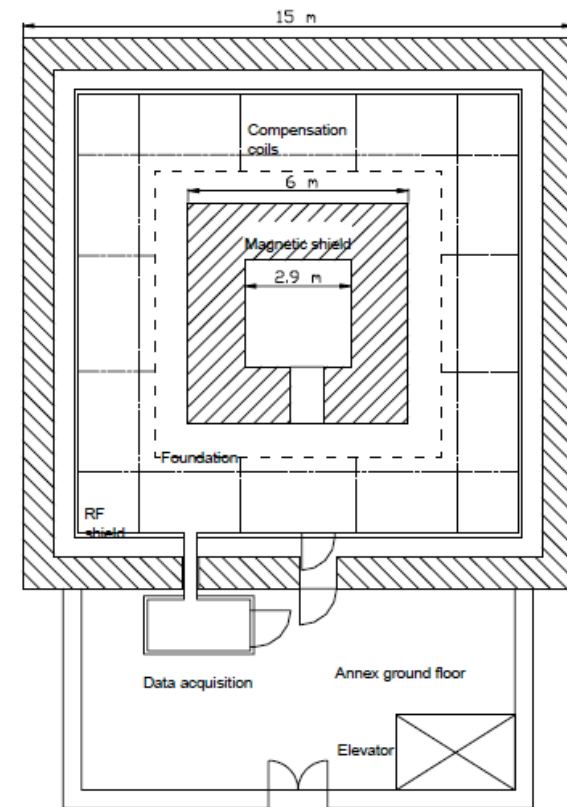


Ambient noise (z-component)



Shielding with passive shields (calculated)

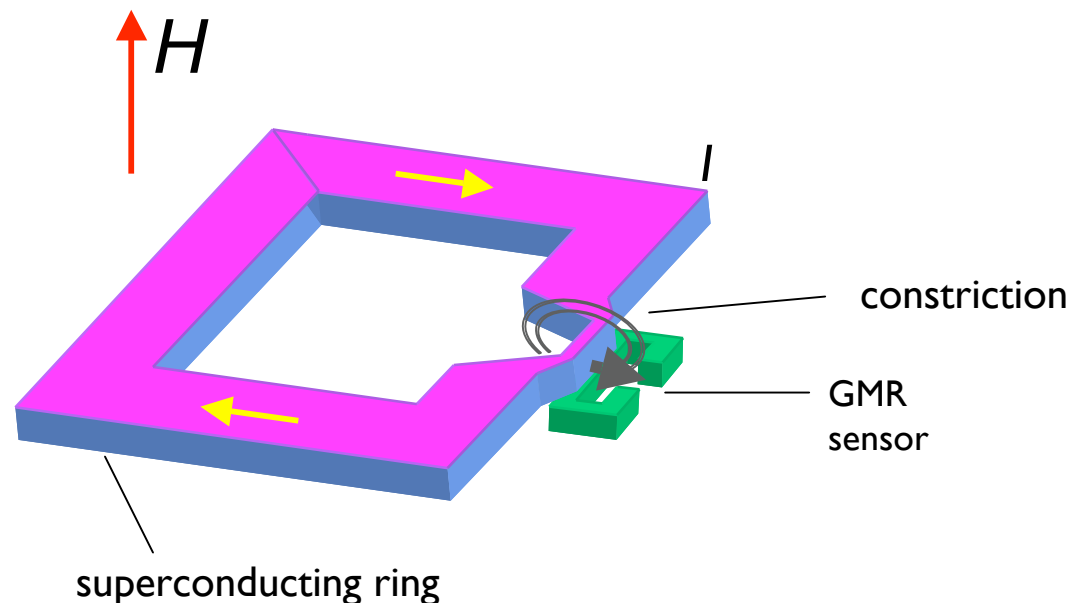
Shielding with active & passive shields (measured)



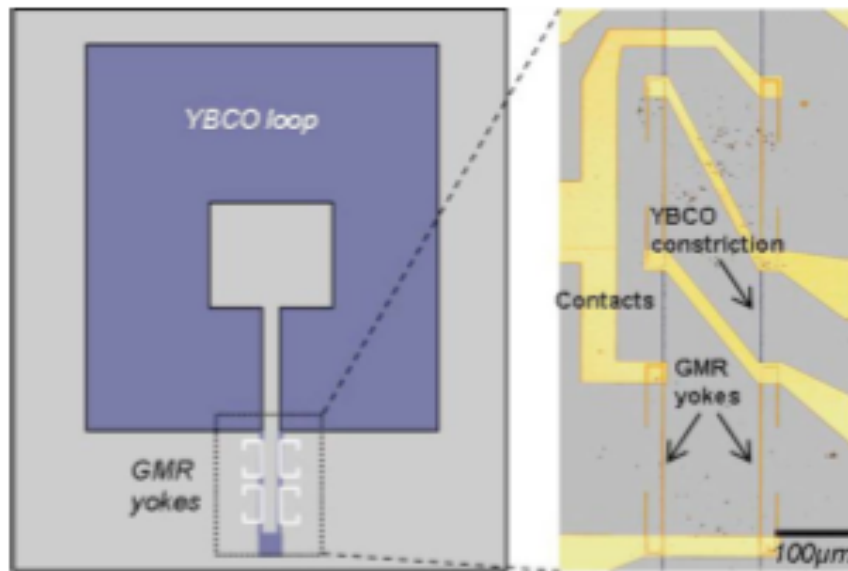
8.3 Mixed Sensor

A hybrid sensor is composed of a superconducting flux to field transformer with a magnetoresistive field sensor.

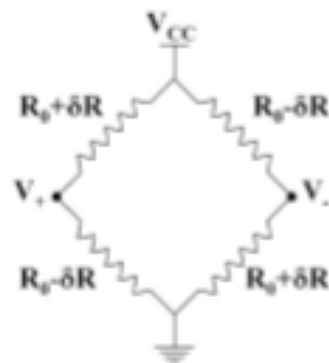
The superconducting loop is made of a low T_c material (Nb) or a high T_c superconductor $\text{YBa}_2\text{Cu}_3\text{O}_7$ (YBCO). It has a narrow constriction where the circulating current in the loop (the flux threading the loop cannot change, so when the applied field increases, so does the screening current flowing in the loop). The current density is high at the constriction where it creates a stray field that is detected by a GMR sensor



The mixed sensor is simpler than a SQUID. A current is induced in the superconducting loop, which is purely passive, in order to exclude flux. Sensitivity approaches the fT level.



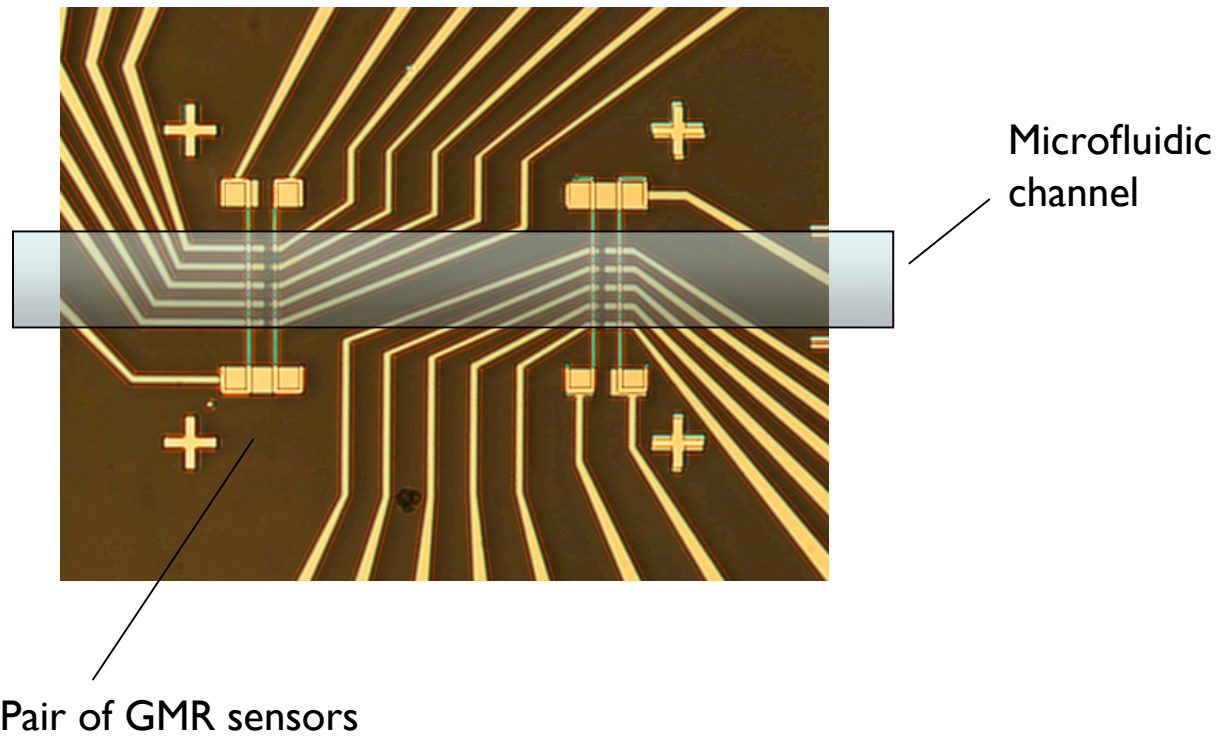
Yoke-type sensors are deposited on the YBCO constriction in a Wheatstone's bridge configuration.



Applications include detection of nmr including NQR of explosives, biomagnetic applications and magnetic imaging.

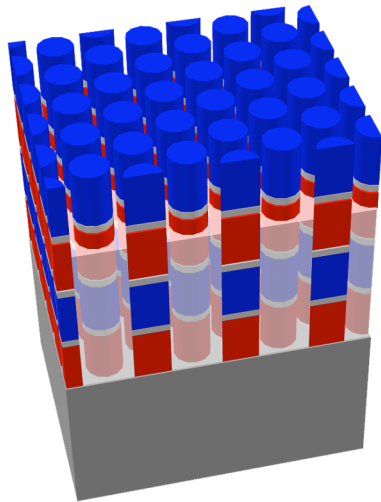
8.4 Magnetic barcodes

Magnetic labels can be detected in microfluidic channels using GMR or TMR spin-valve sensors.



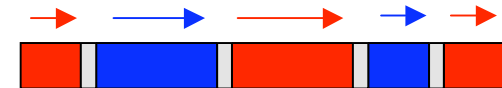


Pulsed-Electrodeposition in nanoporous Al_2O_3

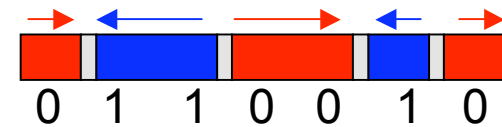


- Hard Ferromagnetic segment
($\text{CoPt}_{\text{hard}}$, $H_{\text{c,hard}} \geq 0.1 \text{ T}$)
- Soft Ferromagnetic segment
($\text{CoPt}_{\text{soft}}$, $H_{\text{c,soft}} \sim 0.05 \text{ T}$)
- Non-Magnetic segment
(Pt)

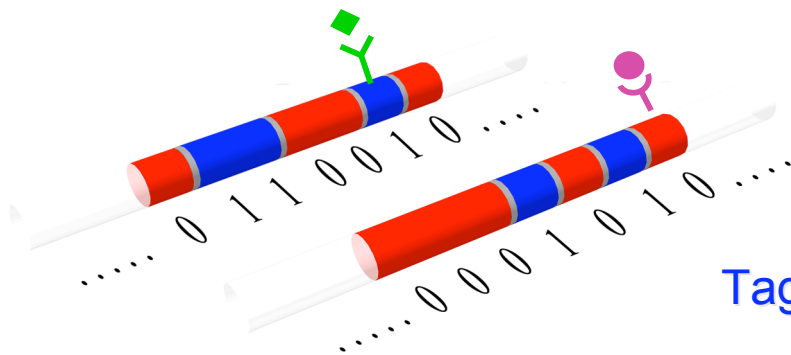
$$H_{\text{appl}} > H_{\text{c,hard}}$$



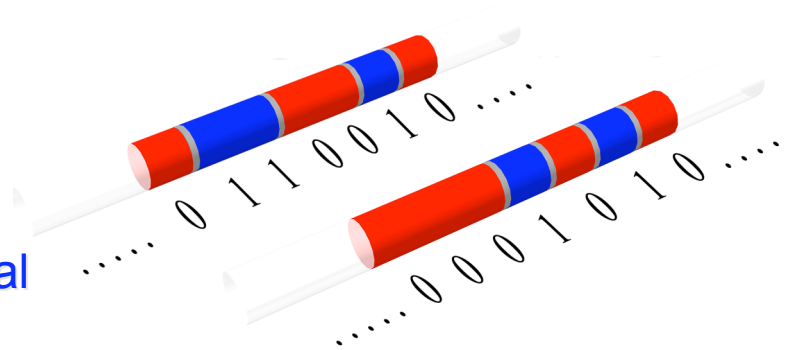
$$H_{\text{c,soft}} < H_{\text{appl}} < H_{\text{c,hard}}$$

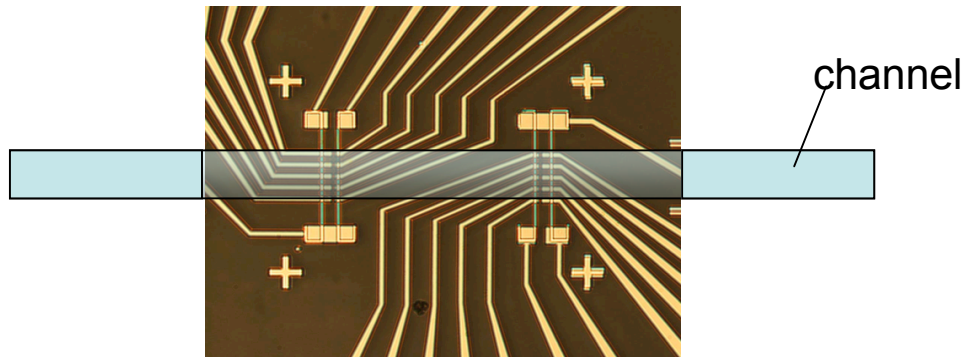


By changing the sequence of the magnetic segments It may be possible to write and storage different codes through the application of magnetic fields

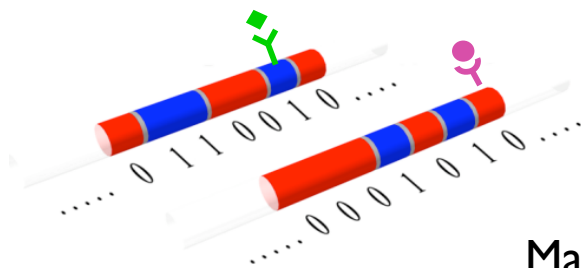


Tagging of biological
molecules



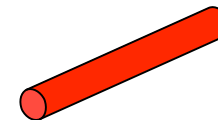
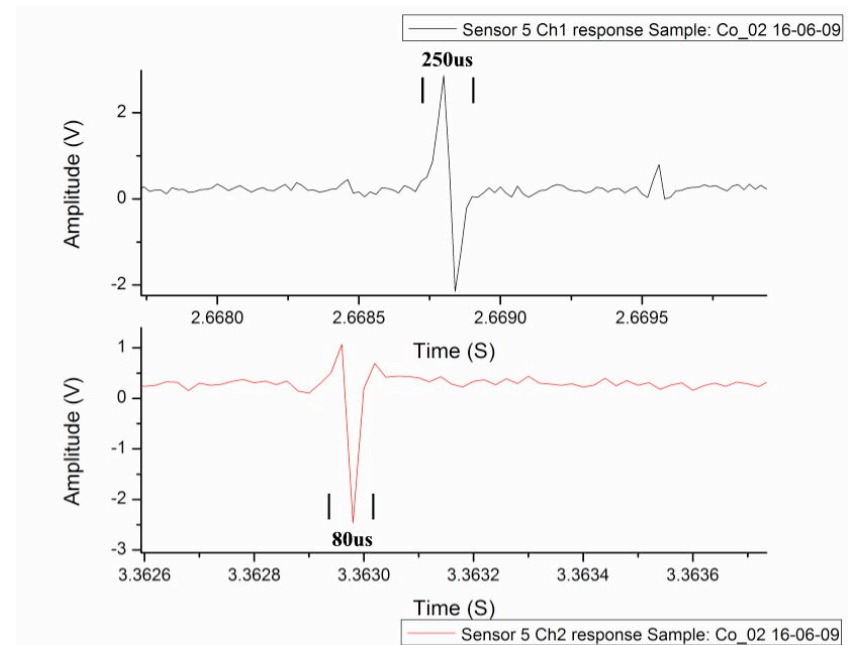


Microfluidic sensor:
Two pairs of yoke-type
spin valve sensors for a
microfluidic channel



Magnetic barcodes

Signals due to *single* nanowire



8.5 Security tags.

Merchandise in stores, books in libraries etc. needs to be labelled with deactivateable tags in order to prevent unauthorized removal.

